Available online at www.sciencedirect.com
ScienceDirect
Journal of the European Ceramic Society 29 (2009) 1595–1602
www.elsevier.com/locate/jeurceramsoc

Rheological properties of alumina feedstocks for the low-pressure injection moulding process

Birgit Loebbecke *, Regina Knitter, Jürgen Haußelt

Forschungszentrum Karlsruhe GmbH, Institute for Materials Research III (IMF III), P.O. Box 3640, 76021 Karlsruhe, Germany

Received 19 June 2008; received in revised form 27 October 2008; accepted 4 November 2008
Available online 13 December 2008

Abstract

The low-pressure injection moulding process (LPIM) allows near-net shape manufacturing of ceramic microcomponents. Feedstocks used in this process have to fulfil different requirements. They have to show good flowability for the machining but they also need to have high solids content to reduce shrinkage during sintering.

This work focuses on the flow behaviour of alumina feedstocks with high solids content, based on two different binder systems and two different alumina powders. By varying particle size, organic binder system, and solids content, the rheological properties of the feedstocks were modified significantly. The material parameters such as viscosity, the derived relative viscosity, and yield stress were investigated systematically. The Herschel–Bulkley model turned out to be suitable for the description of the rheological behaviour of these ceramic feedstocks. The dependency of the relative viscosity on solids content could be well described by models like Krieger–Dougherty, the Eilers, and the Quemada models, while the best results for the maximum packing factors were obtained with the Janardhana Reddy et al. model.

Keywords: Injection moulding; Al_2O_3; Rheology; Plasticity

1. Introduction

In the past 15 years, there has been an increasing trend for miniaturization in nearly all technologies. Developments of new manufacturing methods allow the fabrication of complex, more accurate, and three-dimensional microcomponents made of different materials. Ceramic microstructured components open up new fields of application in microsystem technology and microprocess engineering, especially for high-temperature applications, for which polymer or metal components are not suitable. The ceramic injection moulding process is a near-net shape processing technique that permits manufacturing of complex ceramic microcomponents. It is of great importance to establish a cost-effective manufacturing of a component without reducing the quality of the product.[1] Low-pressure injection moulding (LPIM) provides an excellent option for producing ceramic components using low-cost tools in comparison to high-pressure injection moulding (HPIM).[2]

The role of the feedstocks is of primary importance in the low-pressure injection moulding process. Feedstocks are usually prepared by mixing the ceramic powder with the molten binder system consisting of low-viscous paraffins and waxes. An ideal binder system for ceramic injection moulding must have superior attributes concerning flow characteristics, interaction with powder, debinding and manufacturing.[3,4] The flow properties of the feedstock should permit good rheological behaviour for defect-free moulding[5] that takes place at a temperature of 80 °C and at a pressure of 0.1 MPa in the low-pressure injection moulding machine.

Flow curves of ceramic feedstocks can be described by the Herschel–Bulkley model.[6] This model shows the dependence of the shear stress on the shear rate of the feedstock:

$$\tau = \tau_0 + K\dot{\gamma}^n \quad (1)$$

in which τ is the applied stress, $\dot{\gamma}$ is the shear rate, τ_0 the yield stress, K is the consistency coefficient, and n is the flow behaviour index, with $n < 1$ for pseudoplasticity.

In the literature several mathematical models can be found that describe the relationship between the relative viscosity (η_r) of the suspension and the solids powder content expressed by

* Corresponding author. Tel.: +49 7247 82 6100; fax: +49 7247 82 4612.
E-mail address: birgit.loebbecke@imf.fzk.de (B. Loebbecke).

0955-2219/$ – see front matter © 2008 Elsevier Ltd. All rights reserved.
doi:10.1016/j.jeurceramsoc.2008.11.001

volume fraction (ϕ). The relative viscosity η_r is defined as the quotient of the apparent viscosity of the suspension ($\eta_{feedstock}$) and the pure binder (η_{binder}).

Einstein showed in 1906 that with increasing solids powder content the viscosity of the suspensions increases[7]:

$$\eta_r = 1 + 2.5\phi \tag{2}$$

The Einstein relationship is valid for diluted solutions and requires the solid particles to be spherical with an identical radius.[8–10] Since that time a large number of empirical models have been developed for a correlation of the relative viscosity with high solids content, such as the Krieger–Dougherty model (Eq. (3)),[11] the Eilers model (Eq. (4)),[12] the Quemada model (Eq. 5),[13] and the Janardhana Reddy et al. model (Eq. (7))[1,14]:

Krieger–Dougherty:

$$\eta_r = \left(1 - \frac{\phi}{\phi_{max}}\right)^{-[\eta]\,\phi_{max}} \tag{3}$$

with η_r relative viscosity, ϕ volume fraction, ϕ_{max} maximum packing factor, and $[\eta]$ intrinsic viscosity of the suspension (2.5 for spheres).

Eilers:

$$\eta_r = 1 + \left(\frac{1.25\phi\phi_{max}}{\phi_{max} - \phi}\right)^2 \tag{4}$$

Quemada:

$$\eta_r = \left(1 - \frac{\phi}{\phi_{max}}\right)^{-2} \tag{5}$$

The Eilers model can be modified with a shape factor k after Pahl et al.[15]:

$$\eta_r = 1 + \left(\frac{k\phi\phi_{max}}{\phi_{max} - \phi}\right)^2 \tag{6}$$

with η_r relative viscosity, ϕ volume fraction, and ϕ_{max} maximum packing factor. The shape factor is a measure for the intrinsic viscosity of the suspension and indicates variations from monosized, spherical particles.

Janardhana Reddy et al. model:

$$\eta\phi_b = \eta(\phi_b)_c + \eta_b(1 - (\phi_b)_c) \tag{7}$$

with η feedstock viscosity, ϕ_b binder volume fraction, $(\phi_b)_c$ critical binder volume concentration, and η_b binder viscosity. Note that: $\phi_{max} = (1 - (\phi_b)_c)$.

The viscosity of the suspensions, considering particles as rigid spheres, is directly related to the volume fraction. In suspensions with high-powder concentration, the interactions between the particles affect the overall rheological behaviour. The maximum packing factor ϕ_{max} depends on the arrangement of the particles, which in turn is determined by particle shape, size distribution, and shear flow.[16] ϕ_{max} is the packing factor at which flow is blocked.

Table 1
Alumina powders characteristics.

Al_2O_3 powder	MR52	RC-SP
d_{10} (μm)	0.98	0.37
d_{50} (μm)	1.3	0.54
d_{90} (μm)	1.9	0.71
Specific surface (m^2/g)	6.1	6.6

2. Experimental procedure

The rheological behaviour of four different types of alumina feedstocks for low-pressure injection moulding has been studied. The evaluation of the flowability of different feedstocks was carried out using rheological parameters, such as viscosity and yield stress. The dependence of the shear stress on the shear rate of the feedstock was calculated by the Herschel–Bulkley model. The maximum packing factor ϕ_{max} resulted from rheological mathematical models. Ceramic microcomponents were produced by the low-pressure injection moulding process.

2.1. Materials

Mean particle size and particle size distribution are important for the moulding process. For the dispersion of the ceramic feedstocks, two Al_2O_3 powders were used, MR52 (Martinswerk GmbH, Bergheim, Germany) and RC-SP (Baikowski Malakoff, TX, USA), with d_{50} values of 1.3 and 0.54 μm, respectively. The characteristics of these powders are shown in Table 1. Additionally, two different binder systems were used, a commercially available binder for low-pressure injection moulding Siliplast LP65 (Zschimmer & Schwarz, Lahnstein/Rhein, Deutschland) and a binder consisting of a mixture of paraffin (Sasol Wax GmbH, Hamburg, Germany) and the surface layer-active substance Brij 72 (Fluka Chemie AG, Buchs, Switzerland).

2.2. Plastification

The alumina feedstocks were dispersed at 90 °C by well-dosed addition of previously dried Al_2O_3 powder to the molten binder. A laboratory dissolver of the type Dispermat CA 40-C (VMA Getzmann, Reichshof, Germany) was used for plastification. To minimize component shrinkage, a high solids content of the feedstock was envisaged. For low-pressure injection moulding, however, the feedstocks still need a sufficient flowability. Feedstocks were prepared for each powder–binder compound by mixing the appropriate weight percent of powder and binder. A range of 55.0 vol.% solids content to the specific maximum solids content for each individual system has been covered.

2.3. Rheology

The rheological properties of the feedstocks were analysed with a Physica rotational rheometer MCR 300 (Anton Paar GmbH, Graz, Austria) using a cone-plate measuring system CP

Table 2
Powder–binder systems used to determine the feedstocks viscosity.

System	Al_2O_3 powder	Binder	ϕ_{min} (vol.%)	ϕ_{max} (vol.%)
1	MR52	Siliplast LP65	55.0	77.5
2	MR52	Brij 72/Paraffin	55.0	72.5
3	RC-SP	Siliplast LP65	55.0	69.0
4	RC-SP	Brij 72/Paraffin	55.0	67.0

25-2. The samples were studied in dependence of their solids content at a temperature of 90 °C, and the shear stress was increased up to 1000 or 1500 Pa.

2.4. Low-pressure injection moulding process

Based on a rapid prototyping process chain[17] ceramic microcomponents were produced by combining stereolithography and low-pressure injection moulding. In the first step, the design of the microcomponent was generated as a three-dimensional computer aided design (CAD). Then, the polymer master model was manufactured in a stereolithography facility at envisionTEC (Gladbeck, Germany) in steps of 50 μm with pixel dimensions of 74 μm × 74 μm. On a square plate with a side length of 10 and 20 mm, respectively, the test pattern contains differently inclined or curved geometric patterns like pyramids, spirals, cone structures, and ellipsoid sections. Different rapid prototyping techniques have been described with regard to their suitability to be used as master models in the replication chain[18]. Afterwards the master models were copied into silicone rubber moulds that were directly used as tools for the low-pressure injection moulding process. The filling of the silicone mould usually takes place at a temperature of 80 °C and at a pressure of 0.1 MPa in an injection moulding facility. For the moulding of only a few parts with different feedstocks, however, manual filling of the mould was more reasonable. For this purpose, the feedstock was cast into the mould at a temperature of about 90 °C. To prevent air inclusions the still viscous feedstock was evacuated inside the mould. After cooling down to room temperature the green bodies were carefully demoulded. Subsequently, the green bodies were debindered at 500 °C and sintered for 1 h at temperatures of 1550–1700 °C.

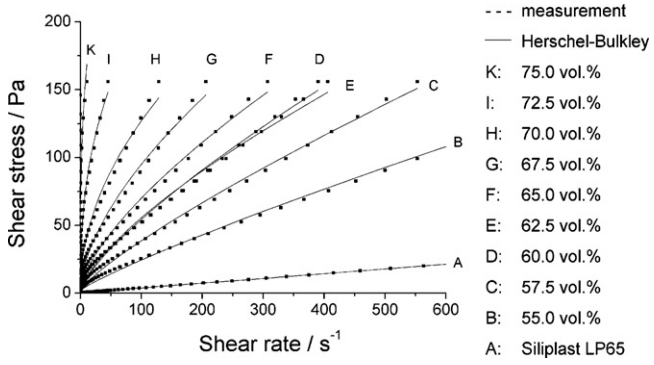

Fig. 1. Flow curves of system 1 (MR52/Siliplast LP65) after Herschel–Bulkley.

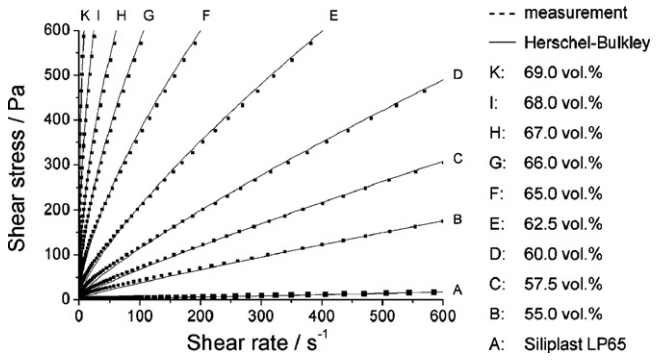

Fig. 2. Flow curves of system 3 (RC-SP/Siliplast LP65) after Herschel–Bulkley.

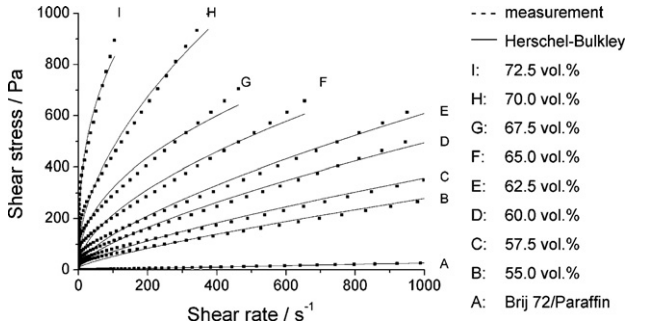

Fig. 3. Flow curves of system 2 (MR52/Brij 72/Paraffin) after Herschel–Bulkley.

3. Results and discussion

3.1. Analysis of flow curves after Herschel–Bulkley

Flow curves of four powder–binder systems consisting of feedstocks having 55.0 vol.% solids content up to the maximum solids content were measured (Table 2). The maximum solids content was experimentally determined as the highest possible solids content before blocking of the flow of the feedstock occurred during feedstock preparation. The highest maximum solids content of 77.5 vol.% was determined for the system MR52/Siliplast LP65 (system 1). Whereas the system RC-SP/Brij72/Paraffin (system 4) with 67.0 vol.% has the lowest maximum solids content. Figs. 1–4 show the flow curves for each powder–binder system. The measured values are charted as dotted lines and the fitted ones with continuous lines. Fitting is based on the Herschel–Bulkley model. All measured

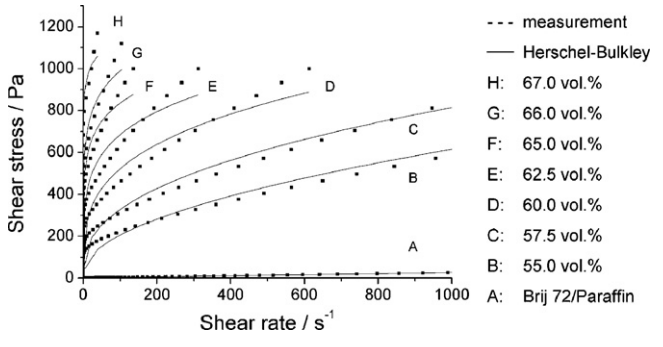

Fig. 4. Flow curves of system 4 (RC-SP/Brij 72/Paraffin) after Herschel–Bulkley.

systems exhibit pseudoplastic behaviour, this means that the viscosity decreases with increasing shear rates. Additionally with increasing solids content of the feedstock the viscosity increases. Feedstocks based on Siliplast LP65 exhibit lower viscosities than feedstocks based on Brij 72/Paraffin at the same solids content. Additionally, viscosities of feedstocks with the Al_2O_3 powder MR52 are lower than viscosities of feedstocks with the powder RC-SP. Higher solids content are possible in feedstocks based on powder MR52, independently of the used binder because of larger powder particles. The viscosity of feedstocks at a solids content of 65 vol.% are for instance 0.7 Pa s for system 1, 2.1 Pa s for system 2, 3.7 Pa s for system 3, and 9.0 Pa s for system 4. Viscosities compared in this work are values at a typical shear rate for low-pressure injection moulding of 100 s^{-1}.

In the following the results of the mathematical analysis via Herschel–Bulkley model are summarized. In case of the RC-SP powder-based mixtures (systems 3 and 4), the yield stress (τ_0) was used as a fixed measured value. In case of MR52 powder-based feedstocks (systems 1 and 2) only mixtures with a solids content larger than 60 vol.% have been considered, because only systems with larger solids content delivered reliable and reproducible data for the yield points. τ_0 was assumed as a variable value for fit approximation for MR52 powder-based feedstocks with a solids content below 62.5 vol.%.

Further measurements have been done to achieve more information about the yield stress at systems 1 and 2 (MR52 powder). For these feedstocks two yield points can be observed at high solids content, which are independent of the used binder. Measured yield stresses have higher τ_0-values for feedstocks based on Brij 72/Paraffin compared to Siliplast LP65 feedstocks, as well as feedstocks based on the finer powder RC-SP have higher yield stresses than those based on coarser powders.

The flow behaviour index n for the pure binder is 0.98 and has nearly Newtonian flow behaviour. With increasing solids content up to the highest maximum solids content the flow behaviour index decreases down to values between 0.37 and 0.42, which indicates pseudoplastic behaviour of the measured feedstocks, and a low index indicates higher shear sensibility.[3,19] For system 4, however, the flow behaviour index n does not show a continuous decrease with increasing solids content. The flow curves based on the binder Brij 72/Paraffin have a more distinct pseudoplastic behaviour than the others. In contrast to the flow behaviour index n, the consistency coefficient K increases with increasing viscosities. The systems based on the binder Siliplast LP65 could be very well described with the Herschel–Bulkley model with correlation coefficients of 0.99, whereas for the binder Brij 72/Paraffin only the system based on MR52 could be sufficiently specified. However, with increasing solids content the fit quality is reduced.

Thomas-Vielma et al. investigated alumina feedstocks for powder injection moulding with powder loadings between 50.0 and 60.0 vol.%.[3] All investigated feedstocks showed pseudoplastic behaviour with flow behaviour index n between 0.50 and 0.56. This flow behaviour index n was expected to allow for a successful ceramic injection moulding avoiding moulding defects.

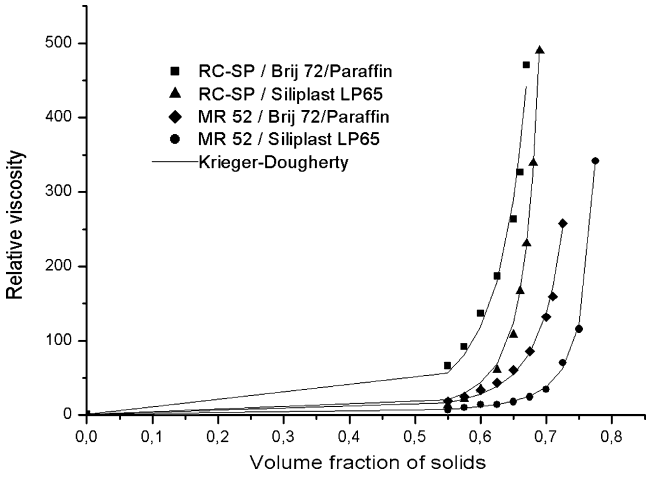

Fig. 5. Relative viscosity versus volume fraction of solids with the use of the Krieger–Dougherty model.

Wei et al. analysed the homogeneity of alumina[20] and zirconia[21] feedstocks for injection moulding with 56.6 and 54.0 vol.% solids content, respectively. In these investigations they determined the flow behaviour index n via power law model. The rheological indexes of two different alumina feedstocks hardly differed (0.27; 0.32–0.38) at the investigated temperatures of 160–180 °C.[20] However, the results of four zirconia feedstocks were not consistent with n values between 0.24 and 0.46.[21] In our investigations the viscosity increased as the flow behaviour index n decreased consistent with the results of viscosity and n given in the literature.

3.2. Determination of the maximum packing factor

The functional dependence of relative viscosity on volume fraction of solids and particle size was determined. Four mathematical models have been studied to estimate the maximum packing factor ϕ_{max}. Fig. 5 shows the experimental data and the simulated curves for each powder–binder system. Fitting is based on Krieger–Dougherty model (Eq. (3) at a shear rate of 100 s^{-1}). The relative viscosity is notably increasing in the systems based on the powder RC-SP at solids content higher than 60.0 vol.%. For the systems based on the powder MR52 this increase appears at 65.0 vol.%. In the feedstocks based on Siliplast LP65 higher solids contents are possible, the relative viscosity is 490 for RC-SP powder (69.0 vol.%) and 342 for MR52 powder (77.5 vol.%). Feedstocks based on MR52 powder have lower viscosities than feedstocks based on RC-SP powder at the same solids content. Therefore, the relative viscosity curves of MR52 progress always below the RC-SP curves. In Table 3 the determined parameter of the powder–binder systems of all fitted models are summarized in comparison to the measured maximum volume fraction. The Krieger–Dougherty model well characterizes the experimental data with correlation coefficients larger than 0.98. But from a practical point of view the resulting coefficients like ϕ_{max} and $[\eta]$ are closer to the expected values for Siliplast LP65 systems than for Brij 72/Paraffin systems. Because of the finer powder the maximum

Table 3
Fitting of four different models at a shear rate of 100 s^{-1}.

Model	Parameter	System 1 MR52/Siliplast LP65	System 2 MR52/Brij 72/Paraffin	System 3 RC-SP/Siliplast LP65	System 4 RC-SP/Brij 72/Paraffin
–	ϕ_m (exp.)	0.775	0.725	0.690	0.670
Krieger–Dougherty	ϕ_{max}	0.810	0.824	0.742	0.849
	$[\eta]$	1.92	2.70	2.45	4.02
	R^2	0.9987	0.9942	0.9966	0.9823
Eilers	ϕ_{max}	0.811	0.796	0.731	0.755
	k	1.00	1.82	1.72	2.97
	R^2	0.9987	0.9965	0.9947	0.9968
Quemada	ϕ_{max}	0.820	0.772	0.722	0.701
	R^2	0.9915	0.9666	0.9805	0.8059
Janardhana Reddy et al.	ϕ_{max}	0.780	0.735	0.692	0.671
	R^2	0.9984	0.9959	0.9989	0.9923

packing factor of 74.2 vol.% of the RC-SP system is lower than 81.0 vol.% of the MR52 system. The fitting for systems based on Brij 72/Paraffin with the same model resulted in too large values for ϕ_{max}.

The intrinsic viscosity $[\eta]$ represents the effective shape factor of the suspended particles for their movement in the shear field imposed.[22] Although ϕ_{max} and $[\eta]$ in Eq. (3) are both significant parameters affected by the degree of agglomeration, in particular $[\eta]$ can be related to the hydrodynamic volume of the suspended particles. Okada and Nagas expected a value of $[\eta] \cong 2.5$ for well-dispersed spherical particles, whereas the value of $[\eta]$ increases with the degree of agglomeration.[22] They showed in rheological investigations of alumina and zirconia powders for injection moulding that the alumina particles in the binder may be in a well-dispersed state and therefore in good agreement with the values ($\phi_{max} = 75.0$ vol.% and $[\eta] = 2.51$) for this system, while the zirconia particles would agglomerate ($\phi_{max} = 66.0$ vol.% and $[\eta] = 3.45$). In addition, the degree of agglomeration for the zirconia particles increased with decreasing volume fraction of solids ($\phi_{max} = 57.0$ vol.% and $[\eta] = 4.21$). This implies that in the mixing process the destruction of the agglomerates due to the grinding of the solid phase in the highly filled system may proceed as the concentration of the powder increases. The used alumina and zirconia powders were nearly spherical particles with mean particle diameters of 0.5 and 0.43 μm, respectively, and identical particle size distributions of 0.1–3 μm.

The intrinsic viscosity $[\eta]$ of the suspended particles in the measured systems based on Siliplast LP65 is 1.92 for MR52 powder and 2.45 for RC-SP powder and indicates well-dispersed particles (Table 3). The Brij 72/Paraffin systems imply an agglomerated state with 2.70 (MR52) and 4.02 (RC-SP). In the densest lattice packing a packing density of 74% can be achieved with regular arrangement of mono-sized spheres. However, with random, real packing densities are in the range of 60–64%. McGeary experimentally achieved a density of 62.5% in one-sized spheres packings.[23] The powders used in this study are not spherical particles, and they have monodisperse distributions (Table 1). As a consequence, higher packing densities of 67.0–77.5 vol.% are possible. This effect can be explained by the particle size distributions. As soon as deviation from ideal spherical particle shape occurs, higher packing densities become possible. Donev et al. have shown that ellipsoidic particles can be randomly packed at higher densities of 68–71%.[24]

Suri et al. investigated agglomerated and deagglomerated tungsten feedstocks for powder injection moulding with solids content of 60 vol.%.[25] They observed in rheological measurements that the feedstock viscosity with agglomerated powder is larger than that of deagglomerated powder. The maximum packing factor for agglomerated powder (63 vol.%) is lower than that of the deagglomerated powder (66 vol.%). Consistent with Okada and Nagas[22] they noticed the same relation between viscosity and packing density of agglomerated particles. The feedstock viscosity (η) as well as the relative viscosity of a system (η_r) increases with an increase in the solids content (ϕ), and decreases with an increase of the maximum packing factor (ϕ_{max}). These variations are expressed by the Krieger–Dougherty equation. An increase in the ratio ϕ/ϕ_{max} affects the feedstock viscosity and the relative viscosity. The term $1 - (\phi/\phi_{max})$ is referred to mobility parameter, which represents the effective space available for suspended particles to move in the medium.[22]

Furthermore, the powder–binder systems were fitted with the modified Eilers model. Fig. 6 shows the experimental data and the simulated curves based on Eq. (6). This model gives the best fits of the experimental data with correlation coefficients larger than 0.994. The calculated maximum packing factor has lower values in Brij 72/Paraffin systems than those from the Krieger–Dougherty model, but the values are still too high compared to the experimental values. The maximum packing factor in system 4 is higher than in system 3, and does not confirm the practical experiences. The shape factor has values between 1.00 and 2.97 and is lower than the intrinsic viscosity from the Krieger–Dougherty model.

Fig. 7 shows the fitting results based on the Quemada model. In comparison to the experiments the maximum packing factors have realistic values. The correlation coefficients are 0.99 and 0.98 for Siliplast LP65 systems, whereas for the Brij 72/Paraffin systems they are only 0.97 and 0.81. The maximum packing factor is approximately 3.0 vol.% higher in systems based on the

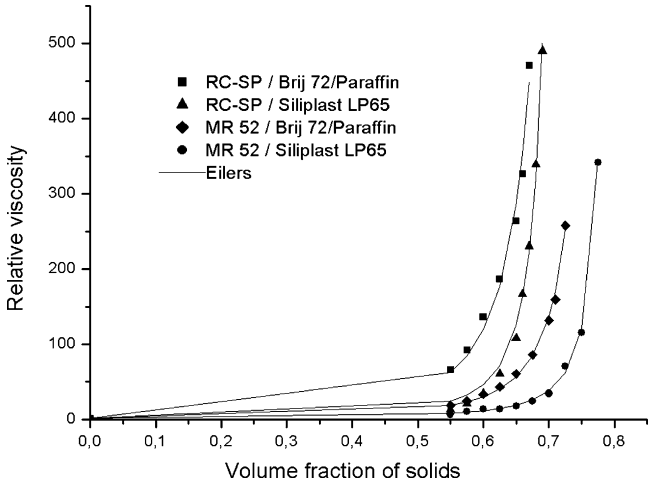

Fig. 6. Relative viscosity versus volume fraction of solids with the use of the Eilers model.

RC-SP powder than the experimentally determined volume fraction, and in systems based on the MR52 powder approximately 4.5 vol.% higher.

A fourth model has been investigated to estimate the maximum packing factor. The Janardhana Reddy et al. (Eq. (7)) fits are simple as they are linear equations rather than exponential functions like the previous models.[14] In Agote et al.[1] six mathematical models have been compared for five highly loaded types of porcelain feedstocks for HPIM, and the Janardhana Reddy et al. model best represents the behaviour of the porcelain powders. Applied to our experimental data, the model gives very realistic values of the maximum packing factor with regression coefficients higher than 0.992. The difference between the calculated and the experimentally determined maximum packing factor of the four powder–binder systems used for LPIM are in all cases smaller than 1 vol.%. The model described by Janardhana Reddy et al.[14] produced the best agreement with our experimental data.

It could be shown that the rheological behaviour of alumina feedstocks is a function of the particle size and shape, solids concentration, and the used binders. ϕ_{max} is strongly dependent

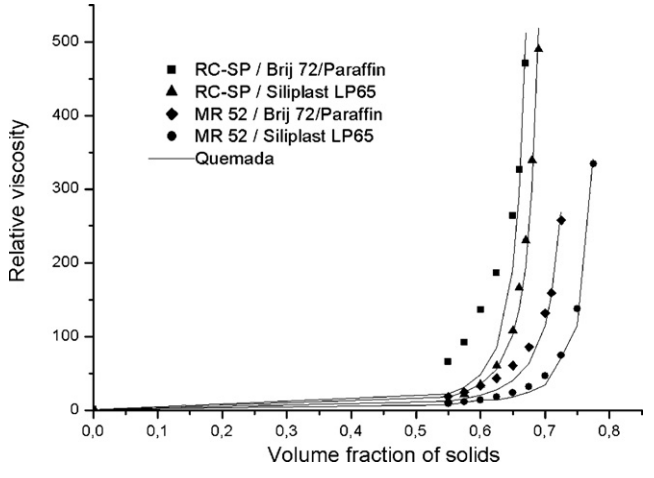

Fig. 7. Relative viscosity versus volume fraction of solids with the use of the Quemada model.

Table 4
Density of sintered parts.

System	Solids content (vol.%)	Sintering temperature (°C)	Density (% th. *D*)
1	75.0	1700	98
	65.0	1700	98
2	65.0	1700	96
3	65.0	1550	97
4	65.0	1550	95

on the feedstock properties and the compaction rate of the used alumina powders. There is a clear dependence of the maximum packing factor on the granulometry of the powder, mean particle size and particle size distribution: the bigger the particle size, the higher the maximum packing factor, quite similar to the conclusions of Agote et al.[1] A broad particle size distribution displays a higher value of the maximum packing factor, because the small particles can fit into the voids between large particles.[26] The correlation coefficients obtained from the Eilers models (Table 3) show the best fitting of the experimental data with values higher than 0.994, but the determined maximum packing factors, especially for the Brij 72/Paraffin system are too high in comparison to the practical experiences. The Janardhana Reddy et al. model best represents the behaviour of the four powder–binder systems at critical loadings with very realistic values of ϕ_{max}.

3.3. Low-pressure injection moulding process

The low-pressure injection moulding process was used in order to confirm the relation between the rheological properties and the injection moulding behaviour of the feedstocks. Feedstocks with viscosities up to 10 Pa s (at a shear rate of 100 s^{-1}) generally turned out to be well suited for the moulding of complex parts. Problems during mould filling were observed using feedstocks with higher viscosity. Using feedstocks with very low solids content, often distortion occurred during debinding of ceramic microcomponents.

Representative results of sintered parts are summarized in Table 4. After sintering, the components exhibited densities between 95% and 98% of the theoretical density and a linear sintering shrinkage of 8–12%. The residual porosity is likely caused by air bubbles entrapped in the feedstock due to the manual filling of the mould. With increasing feedstock viscosity the density of the sintered parts slightly decreases. Sintered parts based on the finer powder RC-SP have a lower sintering temperature than those based on the coarser powder MR52 with comparable sinter densities. The highest solids content at a given viscosity and consequently the lowest shrinkage could be realized with system 1 (MR52/Siliplast LP65).

For the moulding of test pattern, feedstocks with solids content of 65.0 vol.% were used. The sintered ceramic parts were investigated by scanning electron microscopy (SEM) and compared with the master model. In Fig. 8 a detail of the master model – a stepped cone structure – is shown. Figs. 9 and 10 exemplarily show the same detail of the sintered parts with the feedstocks MR52/Brij 72/Paraffin (system 2) and RC-

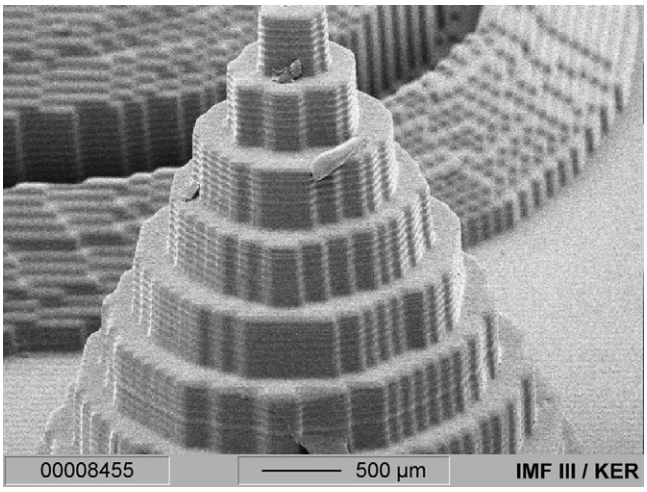

Fig. 8. Detail of the master model from envisionTEC.

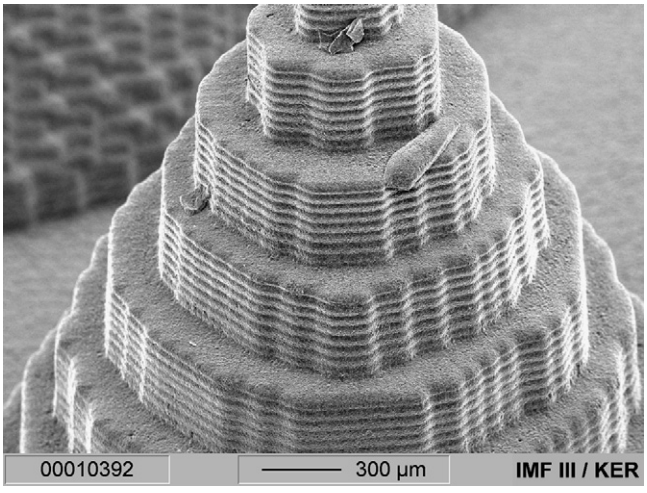

Fig. 9. Sintered alumina – system 2 (65.0 vol.%).

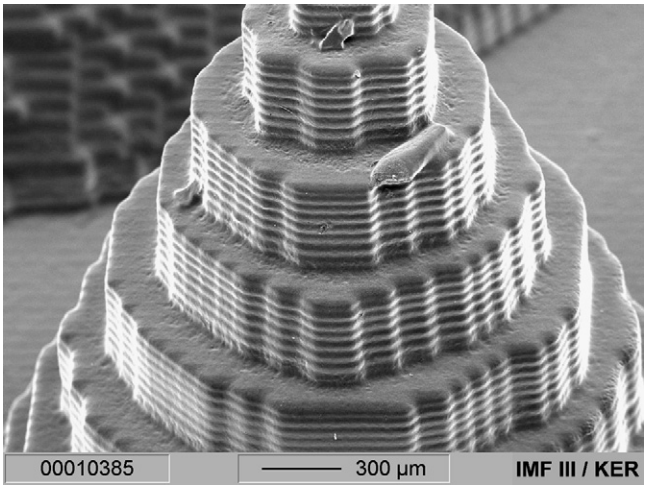

Fig. 10. Sintered alumina – system 3 (65.0 vol.%).

SP/Siliplast LP65 (system 3). The parts made of MR52 powder were sintered at 1700 °C and those made of RC-SP powder at 1600 °C.

Every detail of the master model is very well reproduced into the ceramic components. Defects of the master model were transferred to the silicone tool and subsequently to the green body. Accordingly, the sintered components possess the same defects as the master model. In Fig. 10 the moulded edges of the cone structure are comparable with the master model, whereas in the part of the MR52-ceramic (Fig. 9), the edges are less sharp, due to the higher sintering temperature and the associated grain growth.

4. Conclusions

For the near-net shape manufacturing of ceramic micro-components, the influence of composition on the rheological behaviour of alumina feedstocks was investigated. Feedstocks with high solids content, based on two different binder systems and two different alumina powders, were prepared and their rheological properties were systematically studied. Feedstocks based on the binder Siliplast LP65 exhibit lower viscosities than feedstocks based on Brij 72/Paraffin at the same solids content. With the Herschel–Bulkley model, the systems based on Siliplast LP65 could be very well described, whereas for Brij 72/Paraffin only one system could be sufficiently specified. The flow curves based on Brij 72/Paraffin have more distinct pseudoplastic behaviour than the others. The Janardhana Reddy et al. model best represents the behaviour of the four powder–binder systems with very realistic values of ϕ_{max}. From feedstocks of the powder–binder systems, complex ceramic test pattern with high-moulding precision were manufactured by using a low-pressure injection moulding process.

References

1. Agote, I., Odriozola, A., Gutierrez, M., Santamaria, A., Quintanilla, J., Coupelle, P. *et al.*, Rheological study of waste porcelain feedstocks for injection moulding. *J. Eur. Ceram. Soc.*, 2001, **21**, 2843–2853.
2. Torkar, D., Novak, S. and Novak, F., Apparent viscosity prediction of alumina-paraffin suspensions using artificial neural networks. *J. Mater. Process. Technol.*, 2008, **203**, 208–215.
3. Thomas-Vielma, P., Cervera, A., Levenfeld, B. and Varez, A., Production of alumina parts by powder injection molding with a binder system based on high density polyethylene. *J. Eur. Ceram. Soc.*, 2008, **28**, 763–771.
4. Leverkoehne, M., Coronel-Hernandez, J., Dirscherl, R., Gorlov, I., Janssen, R. and Claussen, N., Novel binder system based on paraffin–wax for low-pressure injection molding of metal–ceramic powder mixtures. *Adv. Eng. Mater.*, 2001, **3**, 995–998.
5. Edirisinghe, M. J. and Evans, G. R. G., Properties of ceramic injection moulding formulations. Part 1. melt rheology. *J. Mater. Sci.*, 1987, **22**, 269–277.
6. Herschel, W. H. and Bulkley, R., Konsistenzmessungen von Gummi-Benzollösungen. *Kolloid-Zeitschrift*, 1926, **39**, 291–300.
7. Einstein, A., Über die von der molekularkinetischen Theorie der Wärme geforderte Bewegung von in ruhenden Flüssigkeiten suspendierten Teilchen. *Ann. Phys.*, 1906, **17**, 549–560.
8. Moreno, R., *Rheology. Encyclopedia of materials: science and technology*. Elsevier Science Ltd., Amsterdam, Netherlands, 2001, pp. 8192–8197.
9. Reed, J. S., *Principles of ceramics processing*. Wiley-Interscience Publication, 1994.

10. Ferraris, C. F., Measurement of the rheological properties of high performance concrete: state of the art report. *J. Res. Natl. Inst. Stand. Technol.*, 1999, **104**, 461–478.
11. Krieger, I. M. and Dougherty, T. J., A mechanism for non-Newtonian flow in suspensions of rigid spheres. *Trans. Soc. Rheol.*, 1959, **3**, 137–152.
12. Eilers, H., Die Viskosität von Emulsionen hochviskoser Stoffe als Funktion der Konzentration. *Kolloid-Zeitschrift*, 1941, **97**, 313–321.
13. Quemada, D., Rheology of concentrated disperse systems and minimum energy dissipation principle. *Rheol. Acta*, 1977, **16**, 82–94.
14. Janardhana Reddy, J., Ravi, N. and Vijayakumar, M., A simple model for viscosity of powder injection moulding mixes with binder content above powder critical binder volume concentration. *J. Eur. Ceram. Soc.*, 2000, **20**, 2183–2190.
15. Pahl, M., Gleißle, W. and Laun, H.-M., *Praktische Rheologie der Kunststoffe und Elastomere*. VDI-Verlag, Düsseldorf, 1991.
16. Zhou, Z., Scales, P. J. and Boger, D. V., Chemical and physical control of the rheology of concentrated metal oxide suspensions. *Chem. Eng. Sci.*, 2001, **56**, 2901–2920.
17. Knitter, R., Bauer, W., Göhring, D. and Risthaus, P., RP process chains for ceramic microcomponents. *Rapid Prototyping J.*, 2002, **8**(2), 76–82.
18. Knitter, R., Bauer, W. and Göhring, D., Microfabrication of ceramics by rapid prototyping process chains. *Proc. Instn. Mech. Engrs. Part C: J. Mech. Eng. Sci.*, 2003, **217**, 41–51.
19. Yang, W.-W., Yang, K.-Y. and Hon, M.-H., Effects of PEG molecular weights on rheological behavior of alumina injection molding feedstocks. *Mater. Chem. Phys.*, 2002, **78**, 416–424.
20. Wei, W.-C. J., Tsai, S. J. and Hsu, K. C., Effects of mixing sequence on alumina prepared by injection molding. *J. Eur. Ceram. Soc.*, 1998, **18**, 1445–1451.
21. Wu, R.-Y. and Wei, W.-C. J., Kneading behaviour and homogeneity of zirconia feedstocks for micro-injection molding. *J. Eur. Ceram. Soc.*, 2004, **24**, 3653–3662.
22. Okada, K. and Nagas, Y., Viscosity and powder dispersion in ceramic injection molding mixtures. *J. Chem. Eng. Jpn.*, 2000, **33**, 168–173.
23. McGeary, R. K., Mechanical packing of spherical particles. *J. Am. Ceram. Soc.*, 1961, **44**, 513–522.
24. Donev, A., Cisse, I., Sachs, D., Variano, E. A., Stillinger, F. H., Connelly, R. *et al.*, Improving the density of jammed disordered packings using ellipsoids. *Science*, 2004, **303**, 990–993.
25. Suri, P., Atre, S. V., German, R. M. and de Souza, J. P., Effect of mixing on the rheology and particle characteristics of tungsten-based powder injection molding feedstock. *Mater. Sci. Eng. A*, 2003, **356**, 337–344.
26. Sigmund, W. M., Bell, N. S. and Bergström, L., Novel powder-processing methods for advanced ceramics. *J. Am. Ceram. Soc.*, 2000, **83**, 1557–1574.